

## Enhanced carrier mobilities in two-dimensional electron gases at III-III/I-V oxide heterostructure interfaces

Valentino R. Cooper\*

*Materials Science and Technology Division, Oak Ridge National Laboratory, Oak Ridge, Tennessee 37831-6056, USA*

(Received 10 November 2011; published 5 June 2012)

Density functional theory is used to explore the electronic reconstruction at III-III/I-V heterointerfaces. It is demonstrated that due to large  $B$ -cation valence differences, a  $\delta$ -doped, two-dimensional electron gas (2DEG) can be created with an increased intrinsic carrier limit, resulting in interfacial charge densities twice that of prototypical  $\text{LaTiO}_3/\text{SrTiO}_3$ . Observed decreases in band effective masses suggest enhancements in carrier mobilities. Unprecedented agreement with recent experiments highlights the fact that it is the electronic structure of the bulk component material that defines the properties of oxide 2DEGs. These geometries provide a more tunable platform through which the underlying physics of electron confinement can be thoroughly examined and thus have implications for modern device applications.

DOI: [10.1103/PhysRevB.85.235109](https://doi.org/10.1103/PhysRevB.85.235109)

PACS number(s): 73.40.-c, 31.15.E-, 71.28.+d, 81.05.Zx

Emergent phenomena at  $ABO_3$  oxide interfaces, e.g., two-dimensional electron gases (2DEGs),<sup>1</sup> are paramount to understanding critical behavior arising from electron confinement, such as metal-insulator transitions,<sup>2</sup> novel magnetic effects,<sup>3</sup> and superconductivity.<sup>4,5</sup> Exploiting these features may be useful in a range of modern technological applications including semiconductor<sup>6</sup> and thermoelectric devices.<sup>7</sup> Furthermore, it has been suggested that the incorporation of heavy,  $5d$ , transition metal elements may result in a significant Rashba spin splitting due to enhanced spin-orbit coupling, a key factor for spintronics.<sup>8,9</sup> Hence, controlling both the mobility and the density of electrons at an interface is crucial for fine tuning these materials for specific device applications as well as providing a foundation for a better understanding of phenomena arising from electron confinement.

A chemically intuitive mechanism, the so-called  $\delta$ -doped mechanism, presents a rich tapestry through which the electronic structure at an interface can be modulated. Here, 2DEGs are a consequence of the presence of multivalent transition metal cations, like Ti, at a heterointerface comprised of  $A$ -site cations with different valence states. For example, in  $\text{LaTiO}_3/\text{SrTiO}_3$  superlattices, the local environment of Ti cations next to a “dopant”  $\text{LaO}$  layer splits the valence of Ti between two possible charge states (+4 for  $\text{SrTiO}_3$  and +3 for  $\text{LaTiO}_3$ ). Therefore, an equal mixture of Ti valence states (3+ or 4+) can be thought to reside at the interface, giving an average valence of 3.5.<sup>10–12</sup> This has been confirmed through electron energy-loss spectroscopy (EELS) measurements<sup>13</sup> in which the distribution of  $\text{Ti}^{3+}$  cations away from the interface was in good agreement with theoretical and experimental carrier density profiles.<sup>14–19</sup> In an ideal system, the extra  $1/2$  electron, relative to Ti in  $\text{SrTiO}_3$ , defines the intrinsic limit of 2DEG carrier densities.<sup>20</sup> This electronic reconstruction is a hallmark of the observed two-dimensional conductivity and is accompanied by polar distortions<sup>15,21,22</sup> (atomic displacements of the cations away from the interface) which effectively screen the electrons near the interfaces. Despite this simple mechanism, to date most commonly studied 2DEGs involve II-IV (primarily  $\text{Sr}^{2+}\text{Ti}^{4+}\text{O}_3$ ) oxides, where the interfacial carrier densities are intrinsically limited to  $0.5 e^-/\text{interface unit cell}$ . Similarly, even fewer

efforts have explored 2DEGs in  $4d$  and  $5d$  transition metals.

In this paper, density functional theory (DFT) calculations are used to investigate the charge rearrangement at interfaces between III-III/I-V perovskites. The guiding principle is that the incorporation of a multivalent cation at an interface, where its desired valence states are +3 and +5, should allow for an average valence of +4, thus increasing the limit of extra interfacial charge to  $1 e^-/\text{interface unit cell}$ . Here, unlike  $\text{LaAlO}_3$ - and  $\text{LaGaO}_3$ -based heterostructures that require multiple layers to create 2DEGs via the polar catastrophe mechanism,<sup>14,23–28</sup> it is demonstrated that it is indeed possible to induce a 2DEG in  $4d$  and  $5d$  superlattices comprised of one layer of  $\text{LaXO}_3$  and seven layers of  $\text{KXO}_3$ , where  $X = \text{Ta}$  and  $\text{Nb}$  without oxygen vacancies.<sup>14,29</sup> More importantly, these heterostructures have a total of one electron per interface unit cell now populating the conduction bands (twice that of a corresponding  $\text{LaTiO}_3/\text{SrTiO}_3$  superlattice). Similar to previous observations, these electrons are primarily confined to  $t_{2g}$  orbitals on  $B$  cations near  $\text{LaO}$  interfaces, decay quickly into the bulk, and are accompanied by large polar ionic distortions. In addition, calculated decreases in electron band effective masses suggest that improved carrier mobilities may be achievable. Remarkable agreement with recent angle-resolved photoemission spectroscopy (ARPES) measurements of surface 2DEG band effective masses<sup>9,30</sup> stresses the point that it is the component material’s electronic structure that defines the interfacial carrier mobilities in oxide 2DEGs.

DFT calculations using the local density approximation (LDA) with a Hubbard  $U$  (LDA +  $U$ )<sup>31</sup> and ultrasoft pseudopotentials<sup>32</sup> as implemented in the QUANTUM ESPRESSO simulation package<sup>33,34</sup> were performed to study 1  $\text{LaXO}_3/7$   $\text{KXO}_3$  superlattices, where  $X = \text{Ta}$  and  $\text{Nb}$ . All superlattice calculations employed an 80 Ry cutoff and an  $8 \times 8 \times 1$   $k$ -point mesh. Comparisons were made with a prototypical 2DEG system, 1  $\text{LaTiO}_3/7$   $\text{SrTiO}_3$ . In all calculations, the in-plane lattice constants were constrained to the theoretical value of the majority component (i.e.,  $\text{KXO}_3$  or  $\text{SrTiO}_3$ ) and the out-of-plane,  $c$ , lattice vector was optimized within the  $P4mm$  space group with  $1 \times 1$  in-plane periodicity. Simultaneously,

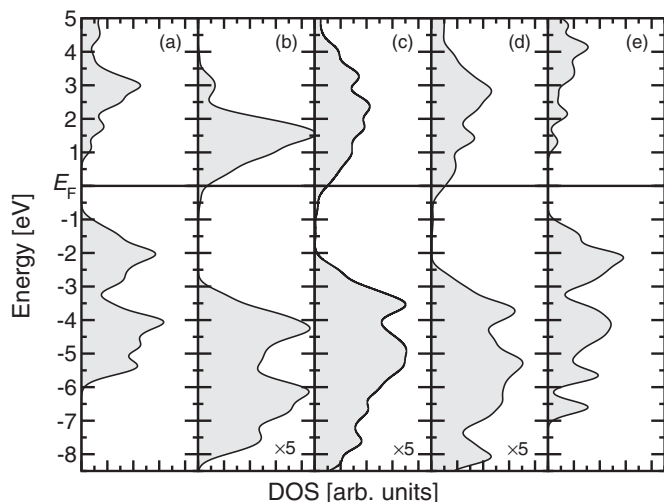


FIG. 1. DOS for (a) bulk SrTiO<sub>3</sub>, (b) 1 LaTiO<sub>3</sub>/7 SrTiO<sub>3</sub>, (c) 1 LaNbO<sub>3</sub>/7 KNbO<sub>3</sub>, (d) 1 LaTaO<sub>3</sub>/7 KTaO<sub>3</sub>, and (e) bulk KTaO<sub>3</sub>. All energies are relative to the Fermi level,  $E_F$ . (The scale for the heterostructures is  $5\times$  that of the bulk structures.)

all ionic coordinates were relaxed until the Hellman-Feynman forces were less than  $8 \text{ meV}/\text{\AA}$ . The computed bulk KNbO<sub>3</sub>, KTaO<sub>3</sub>, and SrTiO<sub>3</sub> cubic lattice constants of  $3.951$ ,  $3.945$ , and  $3.855 \text{ \AA}$ , respectively, are in typical LDA agreement with the experimental values of  $4.000$ ,  $3.988$ , and  $3.901 \text{ \AA}$ , respectively. (Note: these values were obtained using the standard LDA, i.e., without the inclusion of a Hubbard  $U$ .) For all heterostructure calculations, a Hubbard  $U = 5 \text{ eV}$  for  $B$ -cation  $d$  states was found to be appropriate. Similar  $U$  values were used in previous studies of LaTiO<sub>3</sub>/SrTiO<sub>3</sub>.<sup>15,22</sup> For the LaXO<sub>3</sub>/KXO<sub>3</sub> systems, test calculations were also performed for  $U = 3$  and  $8 \text{ eV}$ . All three values of  $U$  yielded essentially the same results (see supplementary figures 1 and 2).<sup>43</sup> Band effective masses were computed using quadratic fits of the partially occupied bands.

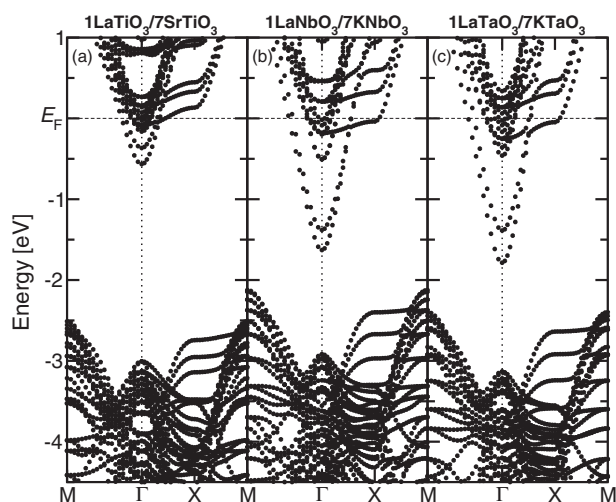


FIG. 2. Electronic band structure for (a) 1 LaTiO<sub>3</sub>/7 SrTiO<sub>3</sub>, (b) 1 LaNbO<sub>3</sub>/7 KNbO<sub>3</sub>, and (c) 1 LaTaO<sub>3</sub>/7 KTaO<sub>3</sub> emphasizing the partially occupied states near the Fermi surface.

Figure 1 depicts the density of states (DOS) for bulk SrTiO<sub>3</sub>, bulk KTaO<sub>3</sub>, 1 LaTiO<sub>3</sub>/7 SrTiO<sub>3</sub>, 1 LaNbO<sub>3</sub>/7 KNbO<sub>3</sub>, and 1 LaTaO<sub>3</sub>/7 KTaO<sub>3</sub> superlattices. Both SrTiO<sub>3</sub> and KTaO<sub>3</sub>, using LDA (i.e., no Hubbard  $U$ ), have relatively large band gaps of  $1.7$  and  $1.8 \text{ eV}$ , respectively. Although smaller than experiment, these are consistent with the LDA's underestimation of oxide band gaps. In agreement with previous studies, 1 LaTiO<sub>3</sub>/7 SrTiO<sub>3</sub> has occupied states just below the Fermi level,  $E_F$ , that sum to 1 electron (or rather  $0.5 e^-$ /interface unit cell).<sup>15</sup> The electronic band structure plot [Fig. 2(a)] indicates that they contribute directly to transport (i.e., cross the Fermi level).

An analysis of the orbital projected DOS indicates that these states are derived mainly from Ti  $t_{2g}$  states, with the two lowest energy, light electron bands coming almost entirely from  $d_{xy}$  orbitals on the interfacial Ti ions and the remaining occupied states being a mixture of  $t_{2g}$  states on all of the Ti cations. More importantly, in 1 LaNbO<sub>3</sub>/7 KNbO<sub>3</sub> and 1 LaTaO<sub>3</sub>/7 KTaO<sub>3</sub>, these occupied electronic states sum up to exactly two electrons (i.e.,  $1 e^-$ /interface unit cell). An examination of the electronic band structure shows that these bands define the Fermi surface [see Figs. 2(b) and 2(c)]. Orbital projected DOSs indicate that they are derived mainly from the  $B$ -cation  $d$  states (Nb/Ta) with dominant electronic contributions arising from partially occupied  $d_{xy}$  orbitals of  $B$  cations at the LaO interface. In all three heterostructures, light electronic bands crossing  $E_F$  are parabolic around  $\Gamma$  and heavy bands extend along the  $\Gamma$ - $X$  direction. This is a characteristic feature of 2DEGs and is consistent with recent ARPES results for 2DEGs at SrTiO<sub>3</sub> and KTaO<sub>3</sub> surfaces.<sup>9,17,30</sup>

Figure 3(a) displays the spatial distribution of the conduction electrons (i.e., arising from states between  $E_F$  and  $\sim -1.8 \text{ eV}$ ) as a function of distance away from the LaO layer. Similar to previous theoretical and experimental results for 2DEGs at heterointerfaces and the SrTiO<sub>3</sub> surface, we find a buildup of charge of roughly  $0.22$  electrons on interfacial Ti cations in the 1 LaTiO<sub>3</sub>/7 SrTiO<sub>3</sub> superlattice.<sup>14-19</sup> (Note: the total atom projected DOS adds up to  $0.95 e^-$  and is scaled to unity in the plots.) This charge quickly decays to  $0.06$  electrons in the center of the slab, indicating a decay length of roughly three to four unit cells. On the other hand, we observe that the LaNbO<sub>3</sub>/KNbO<sub>3</sub> and LaTaO<sub>3</sub>/KTaO<sub>3</sub> heterostructures have a buildup of  $0.52$  and  $0.60 e^-$  on the interfacial Nb and Ta ions, respectively. (Again the projected DOS only sums to  $1.8 e^-$  and is uniformly scaled to  $2.0$ .) Surprisingly, discernible differences in the decay of charge away from the LaO interface are seen. In LaNbO<sub>3</sub>/KNbO<sub>3</sub>, there is still roughly  $0.15 e^-$ /unit cell area in the bulk region, whereas the charge density in LaTaO<sub>3</sub>/KTaO<sub>3</sub> drops off much more sharply, falling to less than  $0.1 e^-$ /unit cell area. This deviation may be linked to the dielectric constants. Model Hamiltonian calculations indicate that larger dielectric constants induce a greater spread of electrons away from the interface.<sup>35,36</sup> KTaO<sub>3</sub> and SrTiO<sub>3</sub> have very similar dielectric constants,<sup>37,38</sup> while KNbO<sub>3</sub> has a much stronger dependence of the dielectric constant on phase.<sup>39</sup> In fact, tetragonal KNbO<sub>3</sub> has a dielectric constant that is a few orders of magnitude greater than SrTiO<sub>3</sub> and KTaO<sub>3</sub>, making the observed behavior reasonable. Regardless, these results clearly indicate a significant enhancement in the concentration of electrons near the interface for a III-III/I-V heterostructure relative to the III-III/II-IV system.

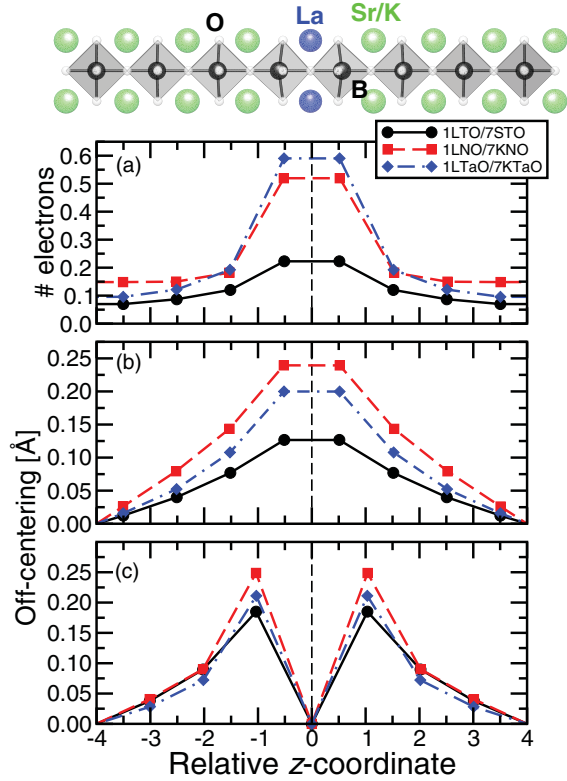


FIG. 3. (Color online) Top: Representative 2D projection of a relaxed superlattices. (a) Charge distribution and (b) magnitude of  $B$ - and (c)  $A$ -cation off-centering as a function of the relative  $z$  coordinate for the superlattices studied. All distances are relative to LaO planes.

In accordance with the observed interfacial electronic reconstruction, we find considerable polar distortions of the  $A$  and  $B$  cations away from the LaO layer. These off-center displacements gradually return to zero in the center of the SrTiO<sub>3</sub> or KXO<sub>3</sub> layers. [See Fig. 3 (top) for a representative 2D projection of the atomic structure of a 1/7 heterostructure.] Similar to previous DFT results, the magnitude of SrTiO<sub>3</sub> off-centering is 0.18 and 0.13 Å for the  $A$  and  $B$  cations near the interface, respectively.<sup>15,22</sup> Figures 3(b) and 3(c) show that the magnitudes of the  $B$ - and  $A$ -cation off-center displacements in the LaXO<sub>3</sub>/KXO<sub>3</sub> structures are all appreciably larger than those in LaTiO<sub>3</sub>/SrTiO<sub>3</sub>. These larger polar distortions are consistent with the need for larger interfacial polarizations to adequately screen the interfacial charges. Unexpectedly, the LaTaO<sub>3</sub>/KTaO<sub>3</sub> superlattice, while having the larger interfacial charge, exhibits smaller polar distortions than LaNbO<sub>3</sub>/KNbO<sub>3</sub>. There are two contributing factors that lead to this discrepancy. First, there is the magnitude of charge screening in these two materials arising from the differences in their respective dielectric constants—with the lower dielectric constant material being more strongly screened and thus requiring smaller ionic distortions. Second, KNbO<sub>3</sub>, unlike KTaO<sub>3</sub>, has a polar ground state which may be more favorable to inducing polar distortions. This is further supported by the fact that the LaTaO<sub>3</sub>/KTaO<sub>3</sub> system retains a cubic average lattice parameter ( $c/a = 1.001$ ), while the LaNbO<sub>3</sub>/KNbO<sub>3</sub> is tetragonally distorted ( $c/a = 1.010$ ; close to the experimental  $c/a = 1.016$ ). The polar nature of the

TABLE I. Structural parameters and relative effective masses for the heterostructures studied.  $a_0$ ,  $c/a$ , and  $m^*/m_e$  denote the cubic lattice parameter, the  $c/a$  ratio, and the relative effective masses of the two lowest energy partially occupied bands, respectively. Note: the curvature of the electronic structure around  $\Gamma$  is symmetric, i.e., the effective mass along the  $\Gamma$ - $X$  and  $\Gamma$ - $M$  directions is essentially equal and thus only one value is reported for each band.

System	$a_0$ (Å)	$c/a$	$m^*/m_e$	
			1	2
1 LaTiO <sub>3</sub> /7 SrTiO <sub>3</sub>	3.885	8.117	0.49	0.59
1 LaNbO <sub>3</sub> /7 KNbO <sub>3</sub>	3.951	8.085	0.35	0.41
1 LaTaO <sub>3</sub> /7 KTaO <sub>3</sub>	3.945	8.009	0.30	0.35

KNbO<sub>3</sub> structure may be more advantageous for controlling interface conductivity through electric field switching.<sup>21,40</sup>

Finally, Table I lists the relative band effective masses,  $m^*/m_e$ , of the two lowest energy partially occupied bands (see Fig. 2). Remarkably, the computed  $m^*$  values for SrTiO<sub>3</sub> are in excellent agreement with ARPES measurements of SrTiO<sub>3</sub> surface 2DEGs (0.5–0.6  $m_e$ ).<sup>30</sup> While the origin of SrTiO<sub>3</sub> surface 2DEGs is attributed to oxygen vacancies, this result is indicative of characteristic electronic structure features. It should be pointed out that La-doped SrTiO<sub>3</sub> has a considerably higher effective mass ( $m^*/m_e > 1$ ) and that the band effective masses predicted here neglect some correlation effects. Moreover, the 1 LaXO<sub>3</sub>/7 KXO<sub>3</sub> structures were found to have significant decreases in  $m^*$  for these bands (which dominate the electron density at the interfaces), implying possible increases in carrier mobilities in the III-III/I-V superlattices. Once again, these values correlate well with recent ARPES experiments for KTaO<sub>3</sub> surface 2DEGs, which measure a band effective mass of 0.30  $m_e$ .<sup>9</sup> This is exceptional agreement, especially when considering the fact that the KTaO<sub>3</sub> surface 2DEG has half the number of electrons as the heterostructures discussed here, and it is indicative of the point that the band effective mass of the oxide 2DEG is an intrinsic property of the bulk component material. Of course, this larger concentration of electrons may lead to decreased mobilities either due to shorter scattering lifetimes,  $\tau$ , or increased electron-electron correlations. However, recently we demonstrated that the carrier mobilities at a  $\delta$ -doped interface may be enhanced through fractional doping (i.e., less than one full doping layer at the interface).<sup>41</sup> The optimal dopant level was found to be 50% for a LaTiO<sub>3</sub>/SrTiO<sub>3</sub> heterostructure. This translates into a 50% decrease in the carrier concentration. As such, optimal fractional  $\delta$  doping of the above structures would allow for much higher carrier concentrations with higher mobilities (coupled to the higher band effective masses). Hence, improvements in electron mobilities,  $\mu_e$ , would be strongly linked to changes in  $m^*$  (where  $\mu_e = e\tau/m^*$ ).

In summary, using first-principles methods, it is demonstrated that superlattices comprising I-V ( $K^{1+}[\text{Nb}/\text{Ta}]^{5+}\text{O}_3$ ) and III-III ( $\text{La}^{3+}[\text{Nb}/\text{Ta}]^{3+}\text{O}_3$ ) perovskites have twice the interfacial charge densities of III-III/II-IV (SrTiO<sub>3</sub>/LaTiO<sub>3</sub>) superlattices. Here, the flexibility of multivalent cations, like Nb and Ta, leads to an intrinsic limit of 1  $e^-$  per interface

unit cell, twice that of previously studied III-III/II-IV and I-V/III-III (Refs. 21 and 42) superlattices. Also, changes in electron band effective masses (with no change in dopant levels) imply that further enhancements in mobilities may be achievable. Correlations between the band effective masses of surface 2DEGs and these heterostructures highlight the characteristic behavior of 2DEGs derived from  $d^0$  transition metal oxides, and a combined approach may be fundamental to understanding the underlying physics of electron confinement.<sup>9,17,30</sup> In addition, deviations in polar distortions indicate that polar, high dielectric constant materials like  $\text{KNbO}_3$  may be more suitable for applications based on electric field switching of interfacial charge-carrier concentrations.<sup>21,40</sup> Naturally, synthetic limitations related to effectively reducing ions like  $\text{Ta}^{5+}$  to  $\text{Ta}^{3+}$  may exist. A feasible route may be to substitute interfacial Ta cations with a cation, like V, that

is more easily reduced. Ultimately, these results present a chemically intuitive framework (in the absence of factors such as O vacancies) through which intrinsic carrier concentrations, and perhaps even carrier mobilities, of oxide heterostructure 2DEGs can be tuned and may be useful in device engineering<sup>6</sup> and in understanding and controlling quantum phenomena due to electron confinement.

V.R.C. would like to acknowledge helpful discussions with C. Bridges, C. Cantoni, H. N. Lee, S. Okamoto, D. Parker, W. Siemons, and D. Xiao. This work was supported by the Materials Sciences and Engineering Division, Office of Basic Energy Sciences, US Department of Energy. This research used resources of the National Energy Research Scientific Computing Center, supported by the Office of Science, US Department of Energy under Contract No. DEAC02-05CH11231.

\*coopervr@ornl.gov

<sup>1</sup>A. Ohtomo, D. A. Muller, J. L. Grazul, and H. Y. Hwang, *Nature (London)* **419**, 378 (2002).

<sup>2</sup>S. Thiel, G. Hammerl, A. Schmehl, C. W. Schneider, and J. Mannhart, *Science* **313**, 1942 (2006).

<sup>3</sup>A. Brinkman, M. Huijben, M. van Zalk, J. Huijben, U. Zeitler, J. C. Maan, W. G. van der Wiel, G. Rijnders, D. H. A. Blank, and H. Hilgenkamp, *Nat. Mater.* **6**, 493 (2007).

<sup>4</sup>K. v. Klitzing, G. Dorda, and M. Pepper, *Phys. Rev. Lett.* **45**, 494 (1980).

<sup>5</sup>T. Ando, A. B. Fowler, and F. Stern, *Rev. Mod. Phys.* **54**, 437 (1982).

<sup>6</sup>J. Mannhart and D. G. Schlom, *Science* **327**, 1607 (2010).

<sup>7</sup>H. Ohta, S. Kim, Y. Mune, T. Mizoguchi, K. Nomura, S. Ohta, T. Nomura, Y. Nakanishi, Y. Ikuhara, M. Hirano, H. Hosono, and K. Koumoto, *Nat. Mater.* **6**, 129 (2007).

<sup>8</sup>S. LaShell, B. A. McDougall, and E. Jensen, *Phys. Rev. Lett.* **77**, 3419 (1996).

<sup>9</sup>P. D. C. King, R. H. He, T. Eknapakul, P. Buaphet, S.-K. Mo, Y. Kaneko, S. Harashima, Y. Hikita, M. S. Bahramy, C. Bell, Z. Hussain, Y. Tokura, Z.-X. Shen, H. Y. Hwang, F. Baumberger, and W. Meevasana, *Phys. Rev. Lett.* **108**, 117602 (2012).

<sup>10</sup>G. A. Baraff, J. A. Appelbaum, and D. R. Hamann, *Phys. Rev. Lett.* **38**, 237 (1977).

<sup>11</sup>W. A. Harrison, E. A. Kraut, J. R. Waldrop, and R. W. Grant, *Phys. Rev. B* **18**, 4402 (1978).

<sup>12</sup>H. Chen, A. M. Kolpak, and S. Ismail-Beigi, *Adv. Mater.* **22**, 2881 (2010).

<sup>13</sup>H. W. Jang, D. A. Felker, C. W. Bark, Y. Wang, M. K. Niranjan, C. T. Nelson, Y. Zhang, D. Su, C. M. Folkman, S. H. Baek, S. Lee, K. Janicka, Y. Zhu, X. Q. Pan, D. D. Fong, E. Y. Tsymbal, M. S. Rzchowski, and C. B. Eom, *Science* **331**, 886 (2011).

<sup>14</sup>W. Siemons, G. Koster, H. Yamamoto, W. A. Harrison, G. Lucovsky, T. H. Geballe, D. H. A. Blank, and M. R. Beasley, *Phys. Rev. Lett.* **98**, 196802 (2007).

<sup>15</sup>S. Okamoto, A. J. Millis, and N. A. Spaldin, *Phys. Rev. Lett.* **97**, 056802 (2006).

<sup>16</sup>S. Okamoto and A. J. Millis, *Nature (London)* **428**, 630 (2004).

<sup>17</sup>A. F. Santander-Syro, O. Copie, T. Kondo, F. Fortuna, S. Pailhes, R. Weht, X. G. Qiu, F. Bertran, A. Nicolaou, A. Taleb-Ibrahimi, P. Le Fevre, G. Herranz, M. Bibes, N. Reyren, Y. Apertet, P. Lecoeur, A. Barthelemy, and M. J. Rozenberg, *Nature (London)* **469**, 189 (2011).

<sup>18</sup>C. Cantoni, J. Gazquez, F. M. Granozio, M. P. Oxley, M. Varela, A. R. Lupini, S. J. Pennycook, C. Aruta, U. S. di Uccio, P. Perna, and D. Maccariello [Adv. Mat. (to be published)].

<sup>19</sup>M. Takizawa, S. Tsuda, T. Susaki, H. Y. Hwang, and A. Fujimori, *Phys. Rev. B* **84**, 245124 (2011).

<sup>20</sup>J. S. Kim, S. S. A. Seo, M. F. Chisholm, R. K. Kremer, H.-U. Habermeier, B. Keimer, and H. N. Lee, *Phys. Rev. B* **82**, 201407(R) (2010).

<sup>21</sup>Y. Wang, M. K. Niranjan, S. S. Jaswal, and E. Y. Tsymbal, *Phys. Rev. B* **80**, 165130 (2009).

<sup>22</sup>D. R. Hamann, D. A. Muller, and H. Y. Hwang, *Phys. Rev. B* **73**, 195403 (2006).

<sup>23</sup>A. Ohtomo and H. Y. Hwang, *Nature (London)* **427**, 423 (2004).

<sup>24</sup>N. Nakagawa, H. Y. Hwang, and D. A. Muller, *Nat. Mater.* **5**, 204 (2006).

<sup>25</sup>R. Pentcheva and W. E. Pickett, *Phys. Rev. Lett.* **102**, 107602 (2009).

<sup>26</sup>N. C. Bristowe, E. Artacho, and P. B. Littlewood, *Phys. Rev. B* **80**, 045425 (2009).

<sup>27</sup>M. Stengel and D. Vanderbilt, *Phys. Rev. B* **80**, 241103 (2009).

<sup>28</sup>P. Perna, D. Maccariello, M. Radovic, U. S. di Uccio, I. Pallecchi, M. Codda, D. Marri, C. Cantoni, J. Gazquez, M. Varela, S. J. Pennycook, and F. M. Granozio, *Appl. Phys. Lett.* **97**, 152111 (2010).

<sup>29</sup>A. Kalabukhov, R. Gunnarsson, J. Börjesson, E. Olsson, T. Claeson, and D. Winkler, *Phys. Rev. B* **75**, 121404 (2007).

<sup>30</sup>W. Meevasana, P. D. C. King, R. H. He, S. K. Mo, M. Hashimoto, A. Tamai, P. Songsirittigul, F. Baumberger, and Z. X. Shen, *Nat. Mater.* **10**, 114 (2011).

<sup>31</sup>V. I. Anisimov, J. Zaanen, and O. K. Andersen, *Phys. Rev. B* **44**, 943 (1991).

<sup>32</sup>D. Vanderbilt, *Phys. Rev. B* **41**, 7892(R) (1990).

<sup>33</sup>M. Cococcioni and S. de Gironcoli, *Phys. Rev. B* **71**, 035105 (2005).

- <sup>34</sup>P. Giannozzi *et al.*, *J. Phys.: Condens. Matter.* **21**, 395502 (2009).
- <sup>35</sup>S. Okamoto and A. J. Millis, *Phys. Rev. B* **70**, 075101 (2004).
- <sup>36</sup>S. S. Kancharla and E. Dagotto, *Phys. Rev. B* **74**, 195427 (2006).
- <sup>37</sup>M. D. Agrawal and K. V. Rao, *J. Phys. C* **3**, 1120 (1970).
- <sup>38</sup>G. Rupprecht and R. O. Bell, *Phys. Rev.* **135**, A748 (1964).
- <sup>39</sup>G. Shirane, H. Danner, A. Pavlovic, and R. Pepinsky, *Phys. Rev.* **93**, 672 (1954).
- <sup>40</sup>A. D. Caviglia, S. Gariglio, N. Reyren, D. Jaccard, T. Schneider, M. Gabay, S. Thiel, G. Hammerl, J. Mannhart, and J. M. Triscone, *Nature (London)* **456**, 624 (2008).
- <sup>41</sup>W. S. Choi, S. Lee, V. R. Cooper, and H. N. Lee (unpublished).
- <sup>42</sup>E. D. Murray and D. Vanderbilt, *Phys. Rev. B* **79**, 100102 (2009).
- <sup>43</sup>See Supplemental Material at <http://link.aps.org/supplemental/10.1103/PhysRevB.85.235109> for the supplementary Figs. 1 and 2.